Semiconductors, Vol. 37, No. 1, 2003, pp. 70–76. Translated from Fizika i Tekhnika Poluprovodnikov, Vol. 37, No. 1, 2003, pp. 70–76.

LOW-DIMENSIONAL SYSTEMS

Lateral Electronic Transport in Short-Period InAs/GaAs Superlattices at the Threshold of Quantum Dot Formation

V. A. Kul'bachinskii*, R. A. Lunin*, V. A. Rogozin*, V. G. Mokerov*, Yu. V. Fedorov*, Yu. V. Khabarov*, E. Narumi, K. Kindo**, and A. de Visser*****

** Moscow State University, Vorob'evy gory, Moscow, 119899 Russia*

*** Osaka University, Japan*

**** Van der Waals–Zeeman Institute, University of Amsterdam, the Netherlands*

Submitted April 8, 2002; accepted for publication April 9, 2002

Abstract—Temperature dependences of resistance at 0.7 K < T < 300 K, the Hall and Shubnikov–de Haas effects in magnetic fields of up to 40 T, photoluminescence (PL), and morphology of a heterointerface (using an atomic-force microscope) of short-period InAs/GaAs superlattices were investigated. The investigations were carried out for a region of subcritical and critical thickness Q = 2.7 monolayers (ML) of InAs. Upon exceeding the critical thickness, the self-organized growth of InAs quantum dots (QDs) set in. The formation of QD layers upon exceeding the critical thickness of InAs Q = 2.7 ML is accompanied by a transition of conductivity from metallic to hopping. It is found that at InAs layer thicknesses of Q = 0.33 ML and Q = 2.0 ML, the PL intensities and electron mobilities in the structures have clearly pronounced maxima. Anisotropy of conductivity, which depends on the thickness of the deposited InAs layers, was observed. © *2003 MAIK "Nauka/Interperiodica".*

1. INTRODUCTION

In recent years, one of most important trends in fundamental and applied solid-state physics has been the investigation of formation of nanostructures resulting from the reconstruction (self-organization) of a surface during heteroepitaxial growth in lattice-mismatched systems. Such processes are observed, for example, in InAs/GaAs semiconductor heterostructures [1–4]. Using these processes, it is possible to obtain, for example, quantum-dot (QD) structures, the investigation of which is of tremendous scientific interest.

The self-organized growth of InAs QDs on a GaAs surface sets in when the thickness of the InAs layer, which is generally measured in monolayers (ML), exceeds a certain critical value. There are numerous publications devoted to the investigation of the optical properties of QD structures. However, the electron-transport properties of InAs/GaAs structures in the region of the critical, and slightly below critical, thickness of the InAs layer are poorly understood.

In this study, the lateral transport of charge carriers in δ-Si-doped short-period InAs/GaAs superlattices is investigated. In essence, these superlattices represent quantum wells (QWs). Investigations were carried out in the region of subcritical and critical thickness of the InAs layers, which is necessary for the formation of the QDs.

2. SAMPLES

The samples investigated were grown by molecular beam epitaxy on semi-insulating GaAs(100) substrates. Each sample consisted of substrate, an undoped GaAs buffer layer 1 μm thick, a short-period InAs/GaAs superlattice (for a detailed description, see below), an undoped $Al_{0.2}Ga_{0.8}As$ spacer 10 nm thick, an Si δ-layer, an $Al_{0.2}Ga_{0.8}As$ layer (35 nm thick), and a GaAs cap layer 6 nm thick (Fig. 1).

The nominal thickness Q of the InAs layers in various superlattices varied from 0.33 to 2.7 ML. The thickness P of the GaAs layers was varied proportionally from 1.7 to 13.5 ML in order to keep the average composition of

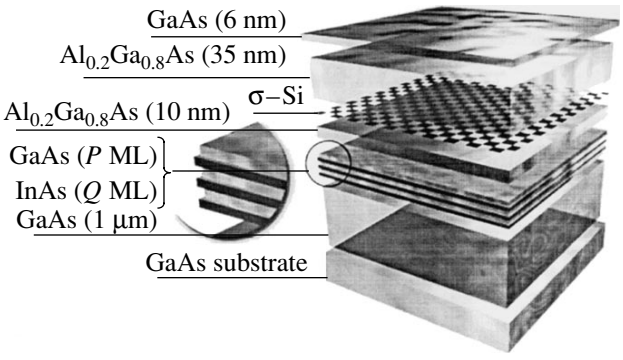

Fig. 1. Schematic representation of the sample structure. Letters P and Q denote the thicknesses of the GaAs and InAs in monolayers (ML), respectively.

Characteristics of the samples investigated

Sample	Q, ML	P, ML	Number of periods N	$h\nu_2$, $h\nu_1$, eV	$\Delta(h\nu_{max})$, meV	E_1–E_0, meV	n_H, 10^{11} cm^{-2}	n, 10^{11} cm^{-2}	μ_H, cm^2/(V s)
				Experiment		Calculation			
1	$In_{0.16}Ga_{0.84}As$ QW			1.434, 1.375	59	50	8.1	8.3	8100
2	0.33	1.7	24	1.419, 1.367	52	54	11.5	–	9400
3	0.67	3.4	12	1.411, 1.369	42	52	7.2	7.0	2060
4	1.00	5.0	8	1.411, 1.370	41	53	7.3	8.7	2450
5	1.33	6.7	6	1.418, 1.374	44	52	8.66	–	4220
6	1.58	8.0	5	1.404, 1.368	36	52	6.8	9.3	4910
7	2.00	10.0	4	1.406, 1.356	50	51	10.4	–	7060
8	2.70	13.5	3	1.390, 1.265	125	–	1.52	–	50

Note: Letters Q and P denote the number of InAs and GaAs monolayers, $h\nu_1$ and $h\nu_2$ are the peak energies of the PL spectrum $h\nu_{max}$ measured at 77 K, $\Delta(h\nu_{max})$ is the difference between the PL peaks, E_1–E_0 is the calculated difference between the electron energy levels, n_H is the Hall electron density, n is the electron density obtained from the Shubnikov–de Haas effect, and μ_H is the Hall mobility. Measurements were carried out at T = 4.2 K.

the superlattice equivalent to the $In_{0.16}Ga_{0.84}As$ solid solution. Such narrow GaAs barriers are penetrable, and, as it will be seen below, the superlattice represents a QW. The number of MLs is not an integer. This means that InAs (or GaAs) is distributed nonuniformly over the structure surface, thus forming separate islands in addition to a continuous layer. Depending on the layer thickness, the number of lattice periods varied from 24 to 3, so that the overall thickness of the superlattice was 14 nm in all of the samples. All superlattices were grown at a temperature T = 490°C, and the other layers were grown at T = 590°C. After the deposition of each InAs layer, the growth was interrupted for 30 s. We investigated eight samples. Some of the parameters of the samples are given in the table.

For comparison, a structure with a single QW was grown (sample 1). In this structure, a layer of $In_{0.16}Ga_{0.84}As$ solid solution was formed instead of a superlattice. This layer had the same thickness of 14 nm.

Data on photoluminescence (PL) (see section 3.3 below) and data obtained by atomic-force microscopy demonstrated that, if the InAs layer thickness exceeded 2.7 ML, then QDs are formed. Figure 2 shows an image obtained using an atomic-force microscope for sample 8 after the selective etching of its upper layers. The InAs islands (i.e., the QDs) are clearly seen.

In this study, we investigated lateral electron transport, i.e., transport over layers of superlattices. To measure the anisotropy of resistance and magnetoresistance, the samples were prepared in the form of L-shaped double Hall bridges using photolithography. The resistance of the structures was simultaneously measured for currents flowing along the [110] direction and along the $[\bar{1}10]$ direction. Magnetoresistance and the magnitude of the Hall effect at low temperatures in magnetic fields of up to 8 T were measured in a superconducting solenoid. A setup at the University of Amsterdam that generated pulsed magnetic fields was used for measurements in magnetic fields of up to 40 T.

3. RESULTS OF MEASUREMENTS AND DISCUSSION

3.1. Temperature Dependences of Resistance

The conductivity of the samples with short-period superlattices was investigated in the temperature range from room temperature to 70 mK (Fig. 3). For the samples with a nominal InAs thickness $Q \le 2.0$ ML, a metallic dependence of resistance on temperature is characteristic. In the region of low temperatures, a logarithmic fall in conductivity, which is characteristic of weak localization of charge carriers, is observed [5]. The absolute value of resistivity for these samples was significantly smaller than h/e^2, which conventionally

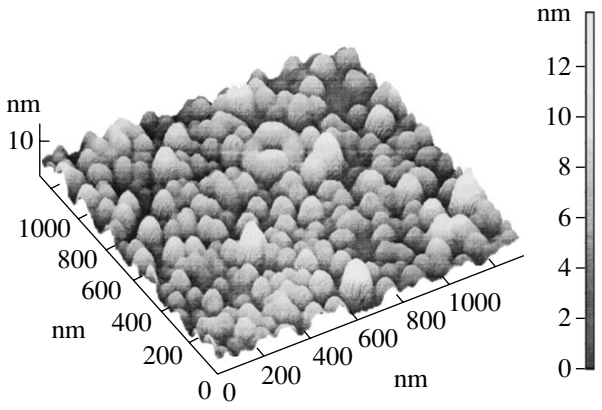

Fig. 2. Atomic-force microscopy image of the QD structure (sample 8) after selective etching of the upper layer.

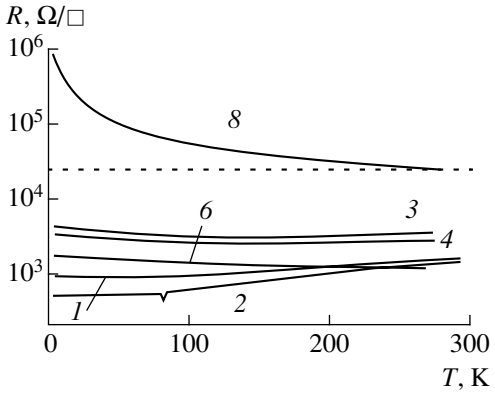

Fig. 3. Temperature dependences of resistance R per area for samples 1–6 with short-period superlattices and sample 8 with QD layers. A horizontal dotted straight line corresponds to the h/e^2 value. Curves are numbered according to sample numbers in the table.

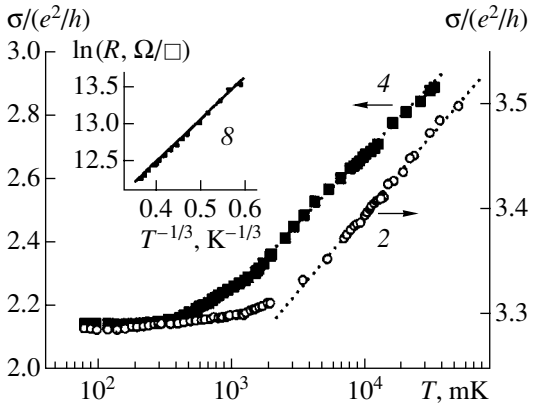

Fig. 4. Conductivity σ for samples 2 and 4 in units of the lowest metallic conductivity e^2/h at low temperatures. The dependence of resistance R on the temperature T for sample 8 in the coordinates corresponding to the Mott law is in the inset. Curves are numbered according to sample numbers in the table.

separates a two-dimensional (2D) metal and insulator. As an example, the temperature dependences of conductivity for samples 2 and 4 are shown in Fig. 4. The temperature scale in Fig. 4 is logarithmic. Due to this, the linear portions are clearly distinguished for each curve as the temperature decreases to ~2 K. At temperatures $T < 1$ K, the conductivity of superlattices with a nominal InAs thickness $Q \le 2.0$ ML levels off (see Fig. 4).

The resistance of sample 8 was larger than h/e^2 in the entire temperature range under consideration and increased as the temperature decreased. At temperatures below 20 K, the resistance was approximated well by a function corresponding to the Mott law for hopping conductivity with a variable hop range for the two-dimensional case. In this case, the approximation takes the form $\rho = \rho_0 \exp[(T_0/T^{1/3})]$ [6] (see inset in Fig. 4). The T_0 parameter for sample 8 equals ~200 K. This parameter is associated with the density of states at the Fermi level and the localization radius as $T_0 = C(g_{E_F} a^2)^{-1}$, where $C = 13.8$ is a numerical coefficient. The localization radius r thus obtained from the experimental data is approximately equal to 53 nm. Hence, a transition from the short-period superlattice to the QD layers upon exceeding the critical InAs concentration is accompanied by a transition from metallic conduction to the hopping one.

3.2. Magnetoresistance and the Shubnikov–de Haas effect

In weak magnetic fields at the liquid-helium temperature, all of the samples showed negative magnetoresistance. For the samples with $Q \le 2.0$ ML, the magnetic-field dependence of negative magnetoresistance was initially quadratic and then logarithmic, which is characteristic of weak localization [5].

In stronger magnetic fields, the Shubnikov–de Haas effect was observed for samples 1–7 with 0 ML $\le Q \le$ 2.0 ML. As an example, Fig. 5 shows the dependences of the magnetoresistance R_{xx} and the Hall resistance R_{xy} for samples 4 ($Q = 1$ ML) and 6 ($Q = 1.58$ ML) in fields up to 40 T. For both samples, clearly distinguishable plateaus in the magnetic-field dependence of R_{xy} are observed. These plateaus correspond to the filling factors of Landau levels $\nu = 1$, 2, and 3. The Fourier spectra of Shubnikov–de Haas oscillations for the same samples are shown in the insets to Figs. 5a and 5b. The presence of a single peak in the Fourier spectra indicates that only the subband of dimensional quantization is filled in the samples under investigation. The electron concentrations n, which were obtained based on the Shubnikov–de Haas oscillations, are given in the table, along with the concentrations n_H and mobilities μ_H obtained from the Hall effect in weak magnetic fields.

3.3. Photoluminescence and Energy Spectrum

Figure 6 shows the PL spectra for sample 1, which contains a single $In_{0.16}Ga_{0.84}As$ QW, and six samples whose superlattices are arranged according to an increase in the InAs layer thickness from $Q = 0.33$ ML to $Q = 2.7$ ML.

As can be seen from Fig. 6, the PL spectra for a sample with a single QW and for samples with superlattices, which contain an InAs layer with a thickness $Q \le$ 2 ML, are shaped similarly. All of these spectra contain two pronounced peaks. The first low-energy peak with a transition energy $h\nu_1$ lies in the range of 1.356–1.375 eV, while the second high-energy peak with a transition energy $h\nu_2$ lies in the range of 1.404–1.434 eV (see

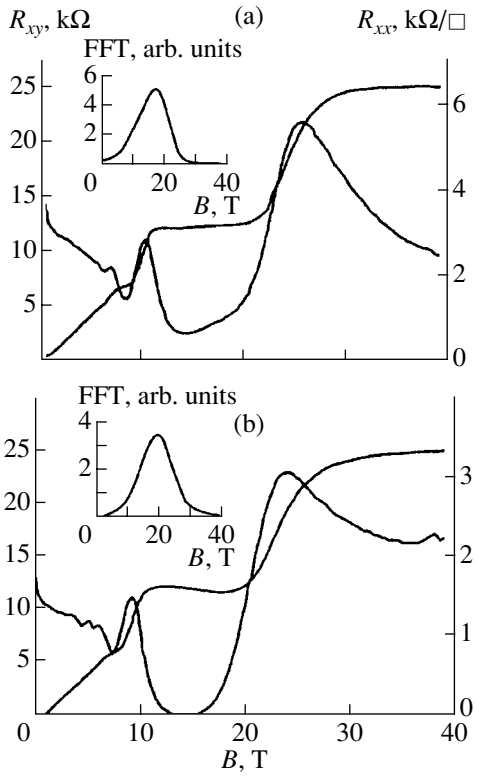

Fig. 5. Transverse magnetoresistance R_{xx} and Hall resistance R_{xy} of samples (a) 4 and (b) 6 at $T = 4.2$ K. Curves are numbered according to sample numbers in the table. The relevant Fourier spectra are shown in inset.

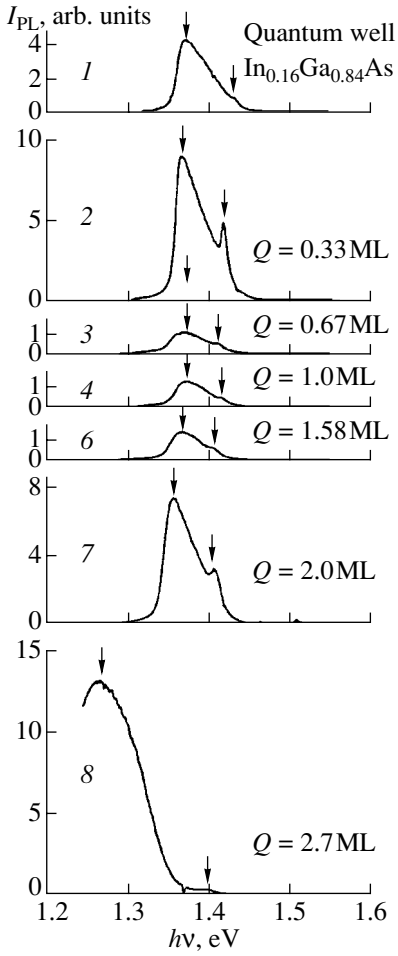

Fig. 6. Photoluminescence spectra of the investigated structures, which differ in the nominal thickness Q of the InAs layers. The scale on the axis of the PL intensity I_{PL} is identical for all drawings. Drawings are numbered according to sample numbers in the table. $T = 77$ K.

table). For all of the samples, the intensity of the first peak is higher than that of the second peak.

Upon reaching a nominal thickness $Q = 2.7$ ML (sample 8) for the InAs layers, radical changes are observed in the PL spectrum (see Fig. 6). A new broad and intense band with a peak at $h\nu = 1.265$ eV emerges in the low-energy region. According to [1], such changes in the spectrum represent a characteristic feature of a transition of an InAs layer from 2D to 3D growth, which leads to the formation of QDs. According to [7], the position of this peak in the PL spectrum allows one to estimate the QD size. In our case, such estimation yields a QD pedestal size of approximately 26 nm.

The electron mobilities μ_H for the samples investigated, which were obtained from the Hall effect, are also given in the table. It is obvious that the variation in the Hall mobility with an increase in the thickness Q of the InAs layers correlates with the Q dependence of the PL intensity I_{PL}. Thus, the mobility for the sample with $Q = 0.33$ ML is highest and equals $\mu_H = 9400$ cm^2/(V s). At $Q = 0.67$ ML, the mobility decreases to 2450 cm^2/(V s); it then increases and attains a value of 7060 cm^2/(V s) at $Q = 2.0$ ML (Fig. 7). For sample 1 with an $In_{0.16}Ga_{0.8}As$ QW, $\mu_H = 8100$ cm^2/(V s).

The results obtained allow us to assume the following. The structure of sample 1, which contains a strained $In_{0.16}Ga_{0.84}As$ QW, is rather homogeneous. In this case, the carrier mobility is determined by scattering, which is characteristic of alloys, and by elastic strains, which are caused by a mismatch of interatomic distances between GaAs and $In_{0.16}Ga_{0.84}As$ [8]. Sample 2 contains less than a single ML of InAs ($Q = 0.33$ ML), and the strains caused by lattice mismatch between InAs and GaAs are small. Due to this, these strains relax at small distances with the resulting formation of a QW. In this QW, scattering and nonradiative recombination are reduced, and the carrier mobility and PL intensity for this sample are highest. Upon reaching a thickness of $Q = 0.67$ ML in the InAs layers, the elastic strains become larger. This probably gives rise to fluctuations in the potential relief and reduces the mobility. A further increase in the thickness of the InAs layers results in a gradual decrease in the elastic strains and fluctuations caused by them, since an increase in the

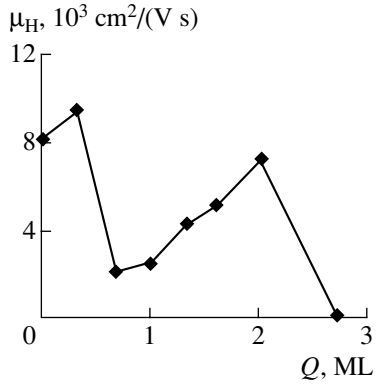

Fig. 7. Dependence of the Hall mobility μ_H on the thickness of the InAs layers (Q) at $T = 4.2$ K. The value $Q = 0$ ML corresponds to sample 1.

carrier mobility and PL intensity is observed with increasing thickness of the InAs layers. The radical reconstruction of the shape of the PL spectrum upon reaching the rated thickness $Q = 2.7$ ML of the InAs layers (sample 8) is indicative of the formation of InAs QDs. A low concentration of free charge carriers in this sample is explained by the localization (see above) of a considerable fraction of electrons in the formed QD arrays, which results in an extremely low Hall mobility in this sample. It is precisely these factors which lead to the nonmonotonic dependence of the PL intensity and the electron Hall mobility on the thickness of the InAs layers.

For all of the samples, the energy spectra and electron wave functions were calculated by the method of the self-consistent solution of the Schrödinger and Poisson equations [9, 10]. In the Schrödinger equation

$$\left[-\frac{\hbar^2}{2}\frac{d}{dz}\left(\frac{1}{m^*(z)}\frac{d}{dz}\right) + U(z)\right]\psi_i(z) = E_i\psi_i(z), \quad (1)$$

the potential energy is expressed by the sum $U(z) = U_H(z) + \Delta U_c + U_{xc}(z)U_H(z)$, where $U_H(z)$ is the electrostatic potential energy, which is determined from the Poisson equation

$$\frac{d}{dz}\left(\varepsilon_0\varepsilon(z)\frac{dU_H(z)}{dz}\right) = e^2[N(z) - n(z)]. \quad (2)$$

Here, $N(z)$ is the bulk concentration of ionized donors,

$$n(z) = \frac{m^*}{\pi\hbar^2}\sum_i (E_F - E_i)\theta(E_F - E_i)|\psi_i(z)|^2 \quad (3)$$

is the electron density at $T = 0$ K, and $\theta(x)$ is the unit-step function. ΔU_c is the offset of the conduction band bottom at the heterojunction, and U_{xc} is the exchange-correlation potential [11]

$$U_{xc} = -\left[1 + 0.0545 r_S \ln\left(1 + \frac{11.4}{r_S}\right)\right]\frac{2}{\pi\alpha r_S}\text{Ry}^*, \quad (4)$$

where

$$\alpha = \left(\frac{4}{9\pi}\right)^{1/3}, \quad r_S = \left(\frac{4\pi a_B^2 n(z)}{3}\right)^{-1/3},$$
$$a_B^* = \frac{4\pi\varepsilon_0\varepsilon\hbar}{m^* e^2}, \quad \text{Ry}^* = \frac{e^2}{8\pi\varepsilon_0\varepsilon a_B^*}. \quad (5)$$

In calculations, band offsets between GaAs layers and strained InAs layers were assumed to equal $\Delta U_c = 535$ meV and $\Delta U_v = 385$ meV [12] for the conduction-band bottom and the valence-band top, respectively. The effective electron mass for the strained InAs layers in the superlattices was assumed to equal $m_c^{st} = 0.0365 m_0$ [13].

As an example, Fig. 8 demonstrates the calculated profiles of the conduction-band bottom (E_c), the positions of two lower electron levels, and the profiles of

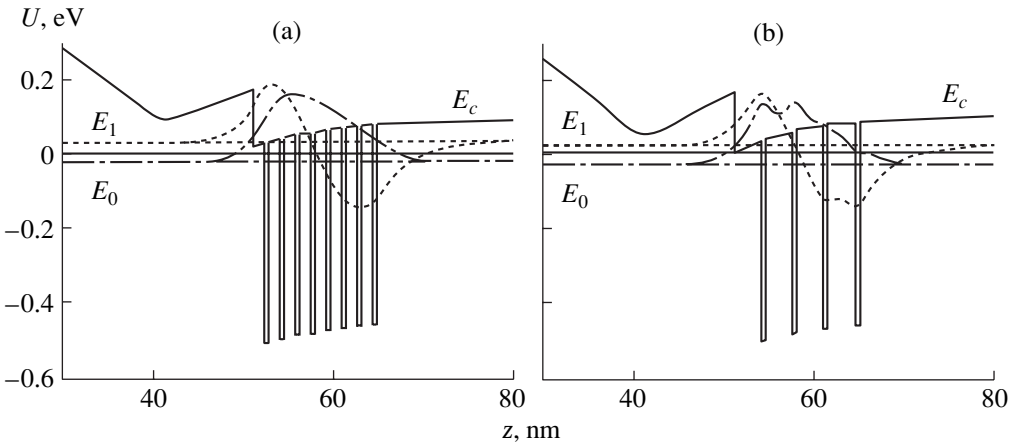

Fig. 8. Calculated profile of the conduction-band bottom (E_c), the position of the lower electron levels E_0 (dash-and-dot line) and E_1 (dashed line), as well as the profile of corresponding wave functions for samples (a) 4 and (b) 7. The letter z denotes the distance from the sample surface. The Fermi level is denoted by a solid horizontal line.

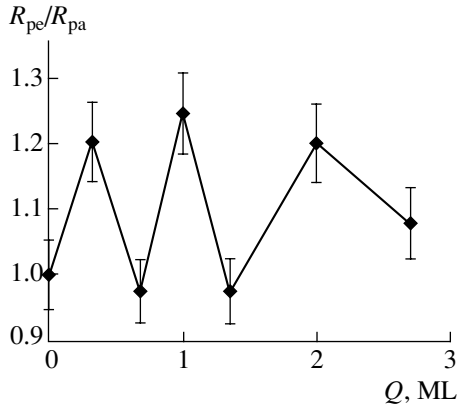

Fig. 9. Ratio of resistance in the [$\bar{1}$10] direction (R_{pe}) to the resistance in the [110] direction (R_{pa}) as a function of the thickness of the InAs layers (Q). The value Q = 0 ML corresponds to sample 1.

wave functions for samples 4 and 7. The Fermi energy is taken as the origin of the energy scale. For all of the samples, only the lower electron levels were occupied with electrons, which corresponds to the data obtained from the Shubnikov–de Haas effect. The calculated difference between the energies of the first and second electron levels is given in the table. It should be noted that the calculated difference between the energies of electron levels is close to the difference between the observed PL peaks. This indicates that it is the first and second electron subbands of dimensional quantization that contribute to the observed transitions.

The configuration of the wave functions in the superlattice for all of the samples resembles the configuration of the wave functions for a single $In_{0.16}Ga_{0.84}As$ QW. It differs from the latter by a modulation which correlates with the profile of the conduction-band bottom of the superlattice. This demonstrates that a short-period superlattice, in essence, represents a QW with profile modulations.

3.4. Anisotropy of Conductivity

For all of the samples, except for sample 1, anisotropy of resistance is observed. Figure 9 demonstrates the dependence of the ratio of resistance in the [$\bar{1}$10] direction to the resistance in the [110] direction on the thickness Q of the InAs layers. The spread of the anisotropy coefficient for a series of samples with the same Q is less than 10%. The anisotropy of resistance correlates with the asymmetry of dislocation distribution [14]. The anisotropy of resistance in a system of 2D electrons is typical of structures with the preferential growth of the deposited material in a single direction [15]. The dependence of anisotropy on the thickness of the InAs layers demonstrates that island growth, which leads to the anisotropy of conductivity, depends on the amount of InAs deposited.

4. CONCLUSION

In this study, the photoluminescence, the temperature dependences of resistance, and the Shubnikov–de Haas effect for short-period InAs/GaAs superlattices, which represent QWs, were investigated. During investigations, magnetic fields up to 40 T were applied in the temperature range of 0.07 K < T < 300 K. An $In_{0.16}Ga_{0.84}As$ QW can be grown as a solid solution or by the sequential fractional deposition of InAs and GaAs layers. In the latter case, at a certain thickness of the deposited InAs layer, specifically, at Q = 0.33 ML and Q = 2.0 ML, the PL intensities and electron mobilities of the structures have clearly pronounced maxima. This is apparently associated with more efficient strain relaxation compared with samples with other values of Q. Anisotropy of conduction is observed, which depends on the thickness of the deposited InAs layers.

It is found that a critical InAs concentration exists (Q = 2.7 ML). At concentrations higher than this value, quantum dots form in the layers. The formation of QDs leads to a sharp decrease in the electron Hall mobility and to a shift of the peak of the PL spectrum. Upon exceeding the critical thickness of the InAs layer, a transition from the short-period superlattice to the QD layer is accompanied by a transition from metallic conduction to hopping conduction with a variable hop range.

ACKNOWLEDGMENTS

This study was supported by the Russian Foundation for Basic Research (project no. 00-02-17493) and by the Ministry of Industry and Science of the Russian Federation.

REFERENCES

1. N. N. Ledentsov, V. M. Ustinov, V. A. Shchukin, *et al.*, Fiz. Tekh. Poluprovodn. (St. Petersburg) **32**, 385 (1998) [Semiconductors **32**, 343 (1998)].
2. D. Bimberg, M. Grundmann, and N. N. Ledentsov, *Quantum Dot Heterostructures* (Wiley, Chichester, 1998).
3. P. W. Fry, I. E. Itskevich, D. J. Mowbray, *et al.*, Phys. Rev. Lett. **84**, 733 (2000).
4. A. D. Yoffe, Adv. Phys. **50**, 1 (2001).
5. T. A. Polyanskaya and Yu. V. Shmartsev, Fiz. Tekh. Poluprovodn. (Leningrad) **23** (1), 3 (1989) [Sov. Phys. Semicond. **23**, 1 (1989)].
6. B. I. Shklovskiĭ and A. L. Efros, *Electronic Properties of Doped Semiconductors* (Nauka, Moscow, 1979; Springer-Verlag, New York, 1984).

7. J.-Y. Marzin, J.-M. Gérard, A. Israël, *et al.*, Phys. Rev. Lett. **73**, 716 (1994).
8. V. A. Kulbachinskii, V. G. Kytin, T. S. Babushkina, *et al.*, J. Low Temp. Phys., Nos. 5/6, 499 (1996).
9. T. Ando, J. Phys. Soc. Jpn. **51**, 3893 (1982).
10. V. A. Kul'bachinskiĭ, R. A. Lunin, V. G. Kytin, *et al.*, Zh. Éksp. Teor. Fiz. **110**, 1517 (1996) [JETP **83**, 841 (1996)].
11. *Theory of the Inhomogeneous Electron Gas*, Ed. by S. Lundqvist and N. H. March (Plenum, New York, 1983; Mir, Moscow, 1987).
12. J. Brübach, A. Yu. Silov, J. E. M. Haverkort, *et al.*, Phys. Rev. B **59**, 10315 (1999).
13. Y. Foulon and C. Priester, Phys. Rev. B **44**, 5889 (1991).
14. T. Schweizer, K. Kohler, W. Rothemund, and P. Ganser, Appl. Phys. Lett. **59**, 2736 (1991).
15. A. de Visser, V. I. Kadushkin, V. A. Kul'bachinskiĭ, *et al.*, Pis'ma Zh. Éksp. Teor. Fiz. **59**, 340 (1994) [JETP Lett. **59**, 363 (1994)].

Translated by N. Korovin